ACS APPLIED MATERIALS & INTERFACES

Research Article

www.acsami.org

Polymeric Micelles Encapsulating Fisetin Improve the Therapeutic Effect in Colon Cancer

Yishan Chen,[†,§] Qinjie Wu,[†,§] Linjiang Song,[†,§] Tao He,[†] Yuchen Li,[†] Ling Li,[†] Weijun Su,[‡] Lei Liu,*[,†] Zhiyong Qian,[†] and Changyang Gong*[,†]

[†]State Key Laboratory of Biotherapy/Collaborative Innovation Center of Biotherapy, West China Hospital, Sichuan University, Chengdu 610041, P. R. China

[‡]School of Medicine, Nankai University, Tianjin 300071, P. R. China

ABSTRACT: The natural flavonoid fisetin (3,3′,4′,7-tetrahydroxyflavone) was discovered to possess antitumor activity, revealing its potential value in future chemotherapy. However, its poor water solubility makes it difficult for intravenous administration. In this study, the monomethyl poly(ethylene glycol)−poly(ε-caprolactone) (MPEG−PCL) copolymer was applied to prepare nanoassemblies of fisetin by a self-assembly procedure. The prepared fisetin micelles gained a mean particle size of 22 ± 3 nm, polydisperse index of 0.163 ± 0.032, drug loading of 9.88 ± 0.14%, and encapsulation efficiency of 98.53 ± 0.02%. Compared with free fisetin, fisetin micelles demonstrated a sustained and prolonged *in vitro* release behavior, as well as enhanced cytotoxicity, cellular uptake, and fisetin-induced apoptosis in CT26 cells. As for *in vivo* studies, fisetin micelles were more competent for suppressing tumor growth and prolonging survival time than free fisetin in the subcutaneous CT26 tumor model. Furthermore, histological analysis, terminal deoxynucleotidyl transferase-mediated nick-end labeling assay, immunohistochemical detection of K_i-67, and microvessel density detection were conducted, demonstrating that fisetin micelles gained increased tumor apoptosis induction, proliferation suppression, and antiangiogenesis activities. In conclusion, we have successfully produced a MPEG−PCL-based nanocarrier encapsulating fisetin with enhanced antitumor activity.

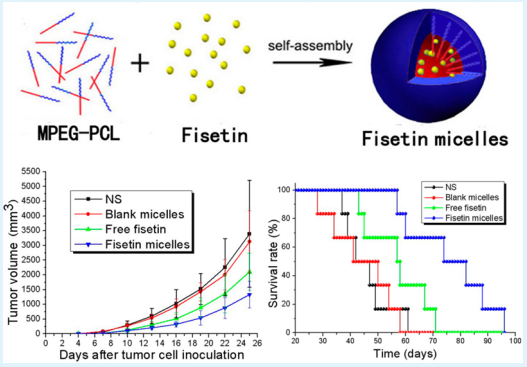

KEYWORDS: *fisetin, micelle, drug delivery, biodegradable, colon cancer*

1. INTRODUCTION

Cancer, the leading worldwide cause of death, is always recognized as a vital target of human medical science. Since chemotherapy became one of the most efficient approaches to reduce the threat of malignancies, many efforts have been made to search for more new antitumor drugs or ameliorate current chemotherapeutic agents. Natural derivatives, once used for disease prevention and treatment in ancient times, made a contribution to the development of modern chemotherapy. For example, it was reported that during 1981−2006 in North America, Europe, and Japan 47.1% of a total of 155 clinically approved anticancer drugs were either unmodified natural products or their synthesized molecules.[1] It should be considered that natural products have a promising future to expand the fields of chemotherapy studies.

Recently, there has been an increasing interest in fisetin (3,3′,4′,7-tetrahydroxyflavone), a natural flavonoid commonly found in fruits, vegetables, nuts, and wine,[2,3] that was discovered to possess various biological properties like antibacterial,[4] antioxidative, anti-inflammatory,[5] and anticonvulsant effects.[6] Molecular targets found related to fisetin include cyclin-dependent kinases, DNA topoisomerases I and II, urokinase, actin polymerization, and androgen receptor signaling.[7] More importantly, the antitumor function of fisetin has been investigated on a range of cancers, such as hepatocellular carcinoma, lung, prostate, pancreatic cancers, as well as colon cancer, confirming the antitumor activity of fisetin. Furthermore, the mechanism of fisetin's antitumor effect was discovered to be associated with antiandrogenic and antimetastatic activities[8,9] and antiangiogenesis.[10] There were studies reporting that fisetin could induce apoptosis in colon cancer cells via certain triggers such as inhibition of COX2 and Wnt/EGFR/NF-κB-signaling pathways or activation of the death receptors and mitochondrial-dependent pathway.[11−13]

However, we cannot ignore the problem that the water solubility of fisetin is poor. Fisetin is hydrophobic, and its water solubility is less than 1 mg/g.[7] Therefore, the difficulties of intravenous administration, low bioavailability, poor selectivity and targeting,[14] or even the toxicity of solvent are all crucial factors for future clinical applications and commercial production.[15] With the help of developing nanotechnology,[16,17] biodegradable polymeric micelles are gradually gaining attention, in the form of drug delivery systems (DDSs),[18,19] to meet these challenges. Polymeric copolymers are nanosized

Received: September 29, 2014
Accepted: December 12, 2014
Published: December 12, 2014

DOI: 10.1021/am5066893
ACS Appl. Mater. Interfaces 2015, 7, 534−542

self-assembled amphiphilic particles, in which the hydrophobic blocks can serve as a container for hydrophobic drugs in the central, and the hydrophilic blocks form a shell contacting with blood components or aqueous solvent.[20] The drug-loaded micelles possess increased antitumor activity and tumor selectivity (passive targeting), due to their sustained release behavior in blood vessels and enhanced permeation and retention effects (EPR effects) in tumor tissues.[21]

In this study, monomethyl poly(ethylene glycol)−poly(ε-caprolactone) (MPEG−PCL) polymeric micelles were chosen, together with fisetin to form a DDS. Fisetin micelles were prepared and characterized. In the following, the antitumor activity of fisetin micelles was investigated both *in vitro* and *in vivo*. The studies of *in vitro* drug release, cytotoxicity, cellular uptake, and *in vitro* apoptosis induction were conducted. *In vivo* antitumor activity of fisetin micelles was later examined in the subcutaneous CT26 tumor model. Furthermore, we took steps to detect the apoptosis, proliferation, and angiogenesis of tumor tissues treated by fisetin micelles.

2. MATERIALS AND METHODS

2.1. Materials. Fisetin (Sigma, USA), monomethyl poly(ethylene glycol) (MPEG, Mn = 2000, Fluka, USA), ε-caprolactone (ε-CL, Alfar Aesar, USA), stannous octoate ($Sn(Oct)_2$, Sigma, USA), Roswell Park Memorial Institute 1640 medium (RPMI 1640, Gibco, USA), thiazoyl blue tetrazolium bromide (MTT, AMRESCO, USA), Hochest33342 (Sigma, USA), propidium iodide (PI, Sigma, USA), and methanol (HPLC grade, Fisher scientific, UK) were used without purification. Other materials were identified as analytic reagent grade and used as received.

MPEG−PCL copolymer was synthesized according to our previous work,[22] and the obtained copolymers were characterized by ^{1}H NMR (molecular weight: 3950).

Mice CT26 and L929 cell lineage were purchased from the American Type Culture Collection (ATCC; Rockville, MD) and cultured in RPMI 1640 supplement with 10% fetal bovine serum (FBS; Caoyuan lvye, Huhht, China). The cell culture was in an incubator with controlled temperature of 37 °C and humidified atmosphere of 5% CO_2.

BALB/c mice (18 ± 2 g), purchased from the Laboratory Animal Center of Sichuan University, were provided with standard laboratory animal living conditions, including laboratory chow and tap water *ad libitum* controlled temperature between 20 and 22 °C, relative humidity of 50%−60%, and 12 h light−dark cycles. Through the process of animal tests, all the mice were treated carefully and humanely following the protocol approved by the Institutional Animal Care and Treatment Committee of Sichuan University (Chengdu, China).

2.2. Preparation and Characterization of Fisetin Micelles. Fisetin and MPEG−PCL micelles (fisetin:MPEG−PCL (wt) = 1:9) were codissolved in dehydrated ethanol under mild stirring. Then, we evaporated the mixed solution with a rotary evaporator at 60 °C, during which fisetin could be distributed in the MPEG−PCL copolymer, and they formed a homogeneous amorphous coevaporation. Finally, the coevaporation was dissolved in a certain volume (dependent on the designed fisetin concentration) of normal saline (NS) at 60 °C so the self-assembly process occurred forming fisetin micelles.

The morphological characteristics of fisetin micelles were evaluated by a transmission electron microscope (TEM, H-6009IV, Hitachi, Japan). The prepared fisetin micelles were diluted with distilled water and put on a copper grid covered with nitrocellulose. Those samples were negatively stained with phosphotungstic acid and dried at room temperature.

The particle size distribution and zeta potential of fisetin micelles were determined by a Malvern Nano-ZS 90 laser particle size analyzer at 25 °C. All the data appeared as mean ± standard deviation (SD, n = 3).

The drug loading (DL) and encapsulation (EE) of fisetin micelles were evaluated according to eqs 1 and 2

$$\mathrm{DL}\ (\%) = \frac{\mathrm{Drug\ (g)}}{\mathrm{Polymer\ (g) + Drug\ (g)}} \times 100\% \quad (1)$$

$$\mathrm{EE}\ (\%) = \frac{\mathrm{Practical\ drug\ loading\ (g)}}{\mathrm{Theoretical\ drug\ loading\ (g)}} \times 100\% \quad (2)$$

The prepared fisetin micelles were lyophilized into powder. Then the powder was weighed and dissolved in methanol. Briefly, the concentration of fisetin in solution was measured by a high performance liquid chromatography (HPLC, Shimadzu LC-20AD, Japan) instrument. The samples were diluted with methanol to reach a proper concentration (10−100 ng/mL) and filtered through a 0.22 μm syringe filter (Millea-LG, Millipore Co., USA) before analysis. Chromatographic separation was performed on a reversed-phase C_{18} column (4.6 mm × 250 mm, 5 μm, WondaSil, Japan) at a temperature of 25 °C. The mobile phase contained 60% (v/v) methanol and 40% (v/v) acidified water (2% (v/v) glactial acetic acid), at a float rate of 1 mL/min. Detection was taken on a diode array detector (SPD-M20A) set at 360 nm. In this way the retention time of fisetin was about 8.8 min. In addition, the standard curve equation was: $H = 26305.578X - 12584.28$ (H: the area of peaks; X: the concentration of fisetin; R^2 = 0.9999).

2.3. *In Vitro* Drug Release Study. The drug release behavior was analyzed in a modified dialysis method.[23] An amount of 1 mL of fisetin micelles and free fisetin (with a fisetin concentration of 1 mg/mL) were placed in dialysis bags (molecular mass cutoff is 3.5 kDa), respectively, which were incubated in 10 mL of prewarmed phosphate-buffered saline (PBS, pH = 7.4, 37 °C) containing 0.5 wt % of Tween80 (for better fisetin dissolution) at 37 °C with gentle shakes at a speed of 100 rpm. At specific points of time, all the release media were collected, stored at −20 °C until analysis, and replaced by prewarmed fresh release media. The concentration of released fisetin in each sample was quantified with HPLC, and tests of each group were performed in triplicate.

2.4. Cytotoxicity of Fisetin Micelles and the MPEG−PCL Copolymer. The cytotoxicity of fisetin micelles and free fisetin was evaluated with the MTT method.[24] CT26 cells were seeded in 96-well plates at a density of 2×10^3 cells per well. After cultured for 12 h, they were exposed to a series of fisetin micelles or free fisetin at gradient concentrations (0−100 μg/mL) for 48 h. In the end, the cell viability was expressed as the mean percentage of cell survival relative to that of untreated cells (n = 6). Furthermore, the cytotoxicity of blank MPEG−PCL micelles on CT26 and L929 cells was also measured in the MTT method mentioned above.

2.5. Cellular Uptake of Fisetin Micelles. The cellular uptake behavior was analyzed using both confocal microscopy and flow cytometric (FCM) analysis. CT26 cells were seeded onto glass coverslips at a density of 1×10^4 cells per well. 24 h later, the growth media were removed, and serum-free media were added into the plates, which, respectively, contained blank micelles (as control), free fisetin, and fisetin micelles. For better detection of the weak florescence, the fisetin concentration used in free fisetin and fisetin micelles was 25 μg/mL, and the MPEG−PCL concentration was 225 μg/mL. After incubation for 0, 2, and 4 h (controlled at 37 °C), the glass coverslips were carefully washed with PBS. To observe the cellular uptake behavior using a confocal microscope (DM6000CS, Leica, Germany), cells were fixed with cold ethanol and stained with Hochest33342. For FCM analysis, CT26 cells were collected and washed with PBS. The intracellular fisetin fluorescence in 10 000 cells was analyzed after being excited with a 488 nm argon laser (BD, USA). Fluorescence emission at 520−530 nm was collected, amplified, and scaled to generate a single parameter histogram (n = 3).

2.6. *In Vitro* Apoptosis Detection. To explore the fisetin-induced apoptosis of CT26 cells, cells at a density of 10×10^4 were plated onto coverslips. After 24 h they were treated with NS, blank micelles (180

DOI: 10.1021/am5066893
ACS Appl. Mater. Interfaces 2015, 7, 534−542

μg/mL), free fisetin (20 μg/mL), and fisetin micelles (20 μg/mL). 48 h later, the growth media were removed, and cells were carefully washed with PBS. In order to observe the cell nuclei, CT26 cells were fixed with cold ethanol, stained with PI, and photographed. Furthermore, the annexin V-PI double staining assay was conducted to quantify the apoptotic level of CT26 cells, using an annexin V-FITC apoptosis detection kit (KeyGen, Nanking, China). The samples of four groups were analyzed with a flow cytometer (BD FACSCalibur, BD, USA), and 10 000 cells were collected for each sample. In the end, the total apoptosis ratio and early/late apoptotic cell ratio were quantified and expressed as mean ± SD (n = 3).

2.7. *In Vivo* Tumor Model and Treatment Plans. To establish the subcutaneous CT26 model, 24 BALB/c mice were subcutaneously injected with 100 μL of CT26 cell suspension containing 5×10^5 cells on day 0. On day 4, when the tumors were palpable, those mice were randomly divided into four groups (n = 6) and were treated with NS (as control), blank micelles (450 mg/kg), free fisetin (50 mg/kg), and fisetin micelles (50 mg/kg) daily for 2 weeks. For each mouse, 100 μL of control or fisetin agent was injected into the tail vein. From day 4 to day 24, the tumor size was measured every 3 days with calipers. The tumor volume was calculated based on the equation vol = $1/2 \times a \times b^2$ (vol: the volume of tumors; a: the length of major axis; b: the length of minor axis). On day 26, mice of four groups were sacrificed by cervical vertebra dislocation. Subsequently, tumors in each group were immediately collected and stored for further analyses. Furthermore, to explore the therapeutic effect of fisetin micelles on extending the lifetime of tumor-bearing mice, another 24 BALB/c mice were divided into four groups and treated with NS, blank micelles, free fisetin, and fisetin micelles as mentioned above, and the survival times were recorded.

2.8. Histological Analysis. Tumor tissues were collected, fixed in 4 wt % paraformaldehyde, embedded in paraffin, and sectioned. After dewaxation and rehydration, sections were stained with hematoxylin and eosin (H&E) to analyze the pathological change of tumor tissues treated with NS, blank micelles, free fisetin, and fisetin micelles.[25]

2.9. Quantitative Assessment of Apoptosis. To conduct the quantitative assessment of apoptosis cells in tumor sections, terminal deoxynucleotidyl transferase-mediated nick-end labeling (TUNEL) staining was used (*in situ* cell death detection kit, Roche, USA) based on the enzymatic addition of digoxigenin-nucleotide to nicked DNA by the recombinant terminal deoxynucleotidyl transferase.[26] Similar high-power fields (five fields for each group) of equal size were chosen to calculate the apoptotic index (the ratio of apoptotic cells to the total number of tumor cells).

2.10. Immunohistochemical Detection of K_i-67. The tumor proliferations were further analyzed by immunohistochemical detection of K_i-67 expression using the labeled streptavidin–biotin method.[27] The primary antibody was rabbit antimouse polyclonal K_i-67 antibody (Millipore, USA), and the secondary antibody was biotinylated goat antirabbit immunoglobulin (ZSGB-BIO, China). Five similar high-power areas for each group were randomly selected to calculate the K_i-67 labeling index (K_i-67 LI, K_i-67 positive/total number of cells), which could quantify the tumor cell proliferation.

2.11. Detection of Microvessel Density (MVD). The antiangiogenesis effect of fisetin micelles could be tested by immofluorescent analysis of neovascularization in tumor tissues.[28] Tumors harvested were cryosectioned and fixed in cold actone, washed with PBS, and stained with rat antimouse CD31 polyclonal antibody (BD Pharmingen, USA). Then they were incubated with Rhodamine (TRITC)-conjugated affinipure goat antirat second antibody (ZSGB-BIO, China). Finally, MVD was evaluated by counting the number of microvessels of the sections in each similar high power field with a fluorescence microscope.

2.12. Statistical Analysis. The statistical analysis was carried out using SPSS 16.0 software. The comparisons of FCM apoptosis rate, tumor weight, and MVD were performed using one-way analysis of variance (ANOVA). As for the heterogeneity of data variance, the comparisons of tumor volume, apoptotic index, and K_i-67 LI were conducted in nonparametric tests. Data of pair groups were analyzed in a Student's t test. Survival curves were generated based on the Kaplan–Meier method, and the statistical significance of them was determined by Mann–Whitney U-tests. A P value <0.05 on a two-tailed test was supposed to be statistically significant.

3. RESULTS

3.1. Preparation and Characterization of Fisetin Micelles. A one-step solid dispersion preparation of fisetin micelles is shown in Figure 1, which could be easily used in

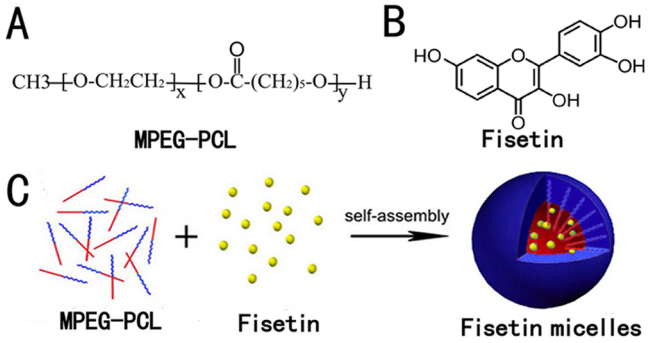

Figure 1. Preparation scheme of fisetin micelles. (A) Chemical structure of MPEG–PCL copolymer. (B) Chemical structure of fisetin. (C) Preparation of fisetin micelles by the self-assembly method.

future scale-up. Fisetin (Figure 1B) could distribute in MPEG–PCL copolymer (Figure 1A) during the evaporation process. Later the coevaporation was dissolved in NS to self-assemble into fisetin micelles.

As Figure 2A presented, the solubility of fisetin in water (b) was poor, while the clear solution of blank micelles (c, 27 mg/mL) and fisetin micelles (d, 3 mg/mL) could be observed, indicating fisetin micelles gained good water solubility. TEM (Figure 2B) demonstrated the spherical shape of fisetin micelles in aqueous solution. The particle size distribution of prepared fisetin-loaded micelles was 22.4 ± 3.0 nm (Figure 1C) with a polydisperse index (PDI) of 0.163 ± 0.032, and the zeta potential was −3.61 ± 0.24 mV (Figure 1D). The particles of fisetin micelles were stable and homogeneous, and the diameter was in good agreement with the results of particle size determination, revealing a very narrow distribution. Moreover, DL and EE were 9.88 ± 0.14% and 98.53 ± 0.02%, respectively.

3.2. *In Vitro* Drug Release Study. As shown in Figure 2E, *in vitro* drug release behavior of free fisetin and fisetin micelles was significantly different. The data suggested that the rate of fisetin released from micelles was much slower in comparison with free fisetin. Within 24 h, the percentage of free fisetin in the outside media was up to 88%, whereas only 56% of fisetin had released from micelles. Then there was a relatively sustained release behavior of fisetin micelles in the following 6 days. At the end of this study, the cumulative release rate of fisetin micelles was 73.58 ± 3.99%, which was much lower than that of free fisetin (92.95 ± 6.51%, $P < 0.05$). This important delay indicated that MPEG–PCL micelles, as an efficient drug carrier, could minimize the exposure of chemotherapeutic agents to normal tissues and increase the accumulation in tumor tissues.

3.3. Cytotoxicity of Fisetin Micelles and the MPEG–PCL Copolymer. MTT assay was conducted to compare the cytotoxicity of free fisetin and fisetin micelles. The data were given as the percentage of viable cells remaining after treatment with a series of fisetin micelles and free fisetin for 48 h. Figure 3A showed both fisetin micelles and free fisetin had significant

DOI: 10.1021/am5066893
ACS Appl. Mater. Interfaces 2015, 7, 534–542

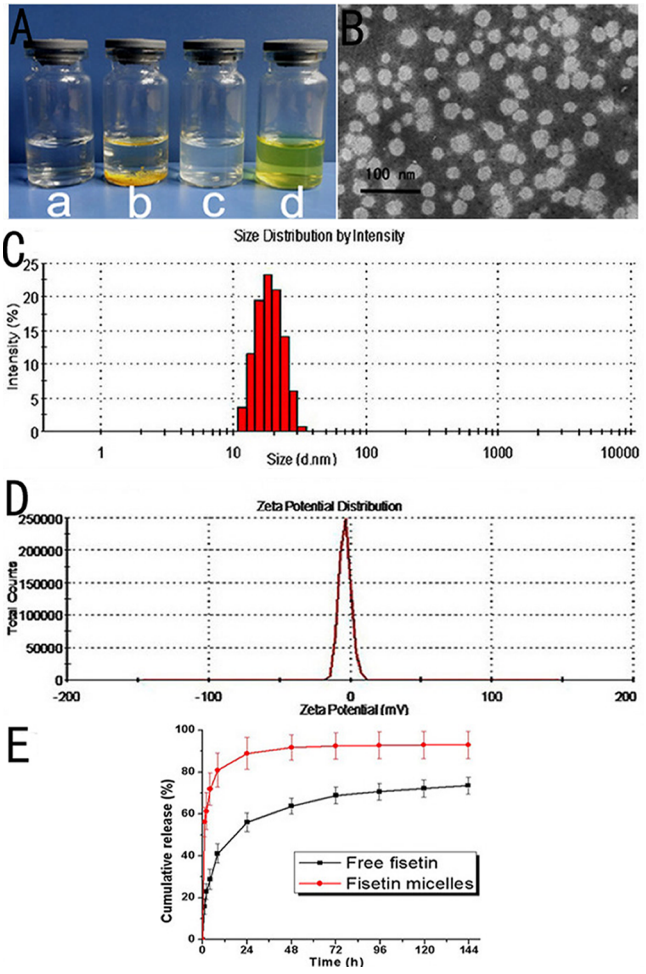

Figure 2. Characterization and *in vitro* release study of fisetin micelles. (A) Morphology of water (a), fisetin in water (b), blank micelles (c), and fisetin micelles (d, the same fisetin amount with b). (B) TEM image of fisetin micelles. (C) Particle size distribution of fisetin micelles. (D) Zeta potential of fisetin micelles. (E) *In vitro* drug release data of free fisetin and fisetin micelles in PBS (containing 0.5 wt % of Tween80, pH = 7.4, 37 °C).

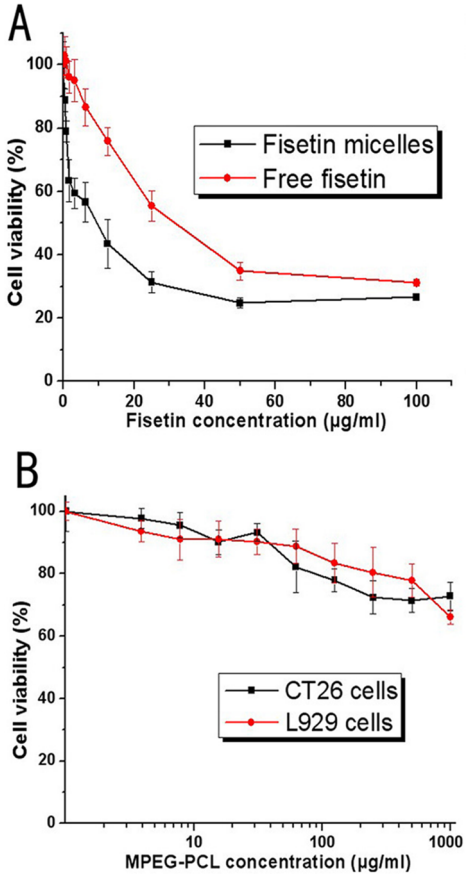

Figure 3. Cytotoxicity studies of fisetin micelles and blank micelles. (A) Cell viability of CT26 cells treated with fisetin micelles and free fisetin for 48 h. (B) Cell viability of CT26 cells and L929 cells treated with blank MPEG−PCL micelles for 48 h.

cytotoxicity against CT26 cells, while half maximal inhibitory concentration (IC50) of fisetin micelles was much lower than that of free fisetin (mean = 7.968 versus 28.513 μg/mL, $P < 0.001$). The results somehow suggested that the encapsulation of fisetin in micelles played an essential role in enhancing the cytotoxicity of fisetin.

The cytotoxicity of blank micelles was evaluated on CT26 and L929 cells, respectively. With increasing concentration of MPEG−PCL micelles, the cell viability decreased, as shown in Figure 3B. When the input concentration of micelles reached 1000 μg/mL, cell viabilities of CT26 and L929 cells were up to 72.13% and 66.13%, respectively, indicating that MPEG−PCL micelles were biocompatible and contained low cytotoxicity, which made it a safe drug carrier.

3.4. Cellular Uptake of Fisetin Micelles. The study of cellular uptake behavior could be visualized using a confocal microscope (DM6000CS, Leica, Germany). The nuclei (stained with Hochest33342) and cytoplasm could be easily distinguished due to the spontaneous green fluorescence of fisetin. Figure 4A presented the images of CT26 cells at 0, 2, and 4 h after treatment with blank micelles (as a control group), free fisetin, and fisetin micelles. Obviously, the cellular uptake was an increasing trend within 4 h because cells observed after 4 h showed a much more bright green fluorescence compared to those observed 2 h earlier. Moreover, the green fluorescence of the fisetin micelles group (both 2 and 4 h incubation) was more distinctive than that of free fisetin, while cells treated with blank micelles did not show any fluorescence until the end, which clarified the nanopackage did not interfere in evaluating the fluorescence of fisetin.

Furthermore, FCM analysis was used to quantify the cellular uptake behaviors. Flow cytometric histograms (Figure 4B) showed that the cellular accumulation of fisetin micelles in CT26 cells was in a relatively higher level compared to that of free fisetin after an incubation of 4 h.

3.5. *In Vitro* Apoptosis Detection. The fisetin-induced apoptosis of CT26 cells was exhibited in Figure 5. Karyopyknosis could be observed in apoptotic cells. In other words, PI-stained nuclei of apoptotic cells would be more condensed, thicker-stained, or even fragmented, different from those of normal cells. In Figure 5A and B, cells in NS and blank micelle groups were in homogeneous tarnished red, and few apoptotic cells existed. Figure 5C and D reported that there was a significant reduction in the number of cells in free fisetin and the fisetin micelles group. Condensed, thick-stained nuclei, fragmented chromatin, as well as apoptotic bodies (shown by arrows) were observed.

Figure 6A presented the double-staining FCM histograms, where the early (Annexin V+/PI−, quadrant 4) and late apoptotic cells (Annexin V+/PI+, quadrant 2) were quantified.

DOI: 10.1021/am5066893
ACS Appl. Mater. Interfaces 2015, 7, 534−542

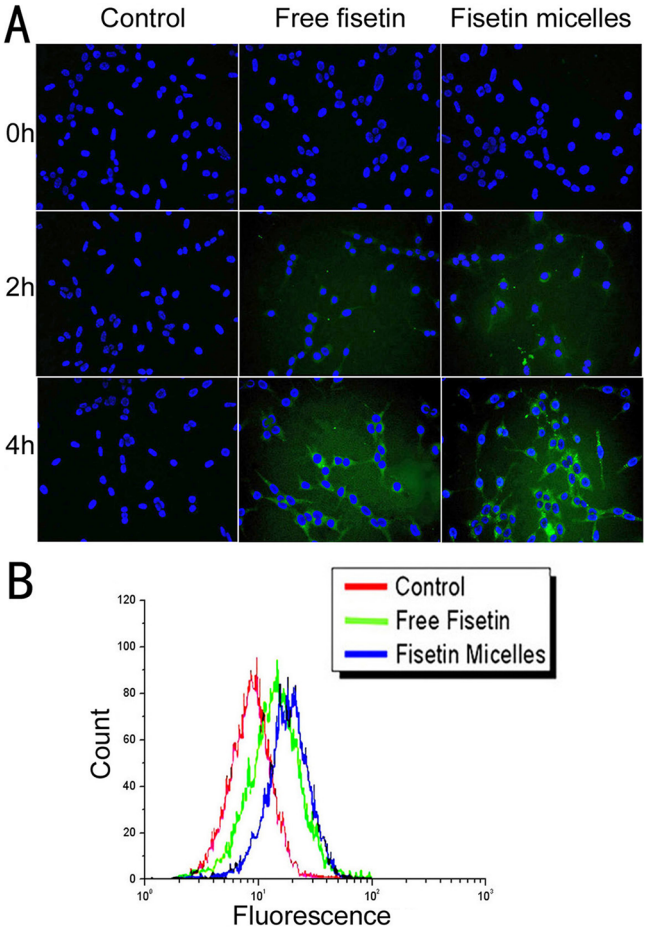

Figure 4. Cellular uptake studies of fisetin micelles. (A) Representative fluorescent images of CT26 cells treated with blank medium, blank micelles, free fisetin, and fisetin micelles under a confocal microscope at specific time (cell nuclei were stained with Hochest33342, and the green fluorescence inside the cytoplasm indicated the cellular distribution of fisetin micelles). (B) Flowcytometric histograms for fisetin micelles and free fisetin accumulating in CT26 cells for 4 h.

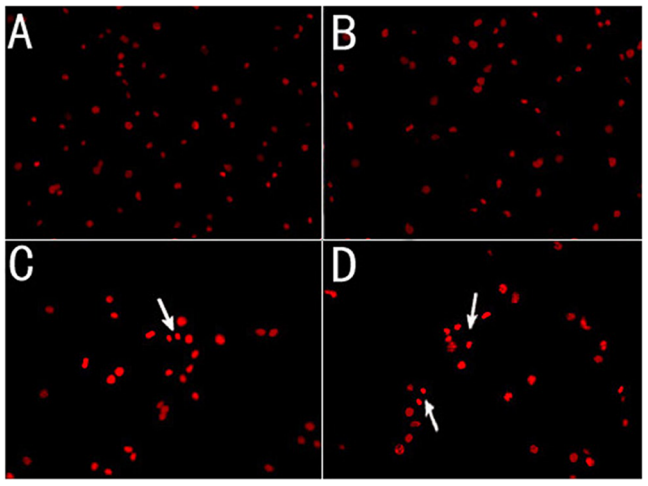

Figure 5. Representative images of CT26 cells treated with NS (A), blank micelles (B), free fisetin (C), and fisetin micelles (D) for 48 h. Cell nuclei were stained with PI, and arrows point to the apoptotic body.

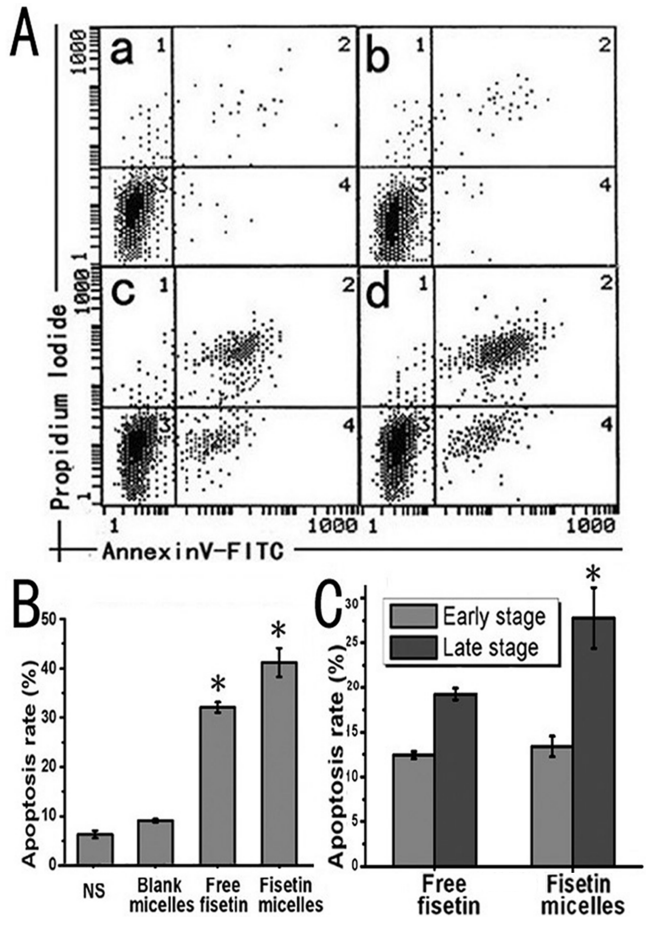

Figure 6. Quantitative determination of fisetin-induced apoptosis in CT26 cells. (A) Representative images of double staining FCM histograms of NS (a), blank micelles (b), free fisetin (c), and the fisetin micelles group (d) (quadrant 1: Annexin V−/PI+; quadrant 2: Annexin V+/PI+, late apoptosis; quadrant3: Annexin V−/PI-; quadrant 4: Annexin V+/PI−, early apoptosis). (B) The apoptosis rate in each group. (C) The rate of early and late apoptosis in free fisetin and the fisetin micelles group.

As shown in Figure 6B, the total apoptosis rates of free fisetin (32.07 ± 1.06%) and the fisetin micelle group (41.17 ± 2.90%) were significantly higher than that of the NS group (6.33 ± 0.77%, $P < 0.001$). The blank micelles group (9.09 ± 0.35%) was not determined as different from the NS group ($P > 0.05$). In addition, fisetin micelles showed more efficient apoptosis induction than free fisetin ($P < 0.05$). Figure 6C demonstrated the comparison of the early and late apoptosis rate of free fisetin and the fisetin micelles group. In the early apoptosis stage, there was no significant divergence in fisetin micelles and free fisetin ($P > 0.05$). As for late apoptosis, the rate of the fisetin micelles group was larger than that of the free fisetin group (mean apoptosis rate = 19.64 ± 0.65 vs 27.77 ± 3.41%, $P < 0.05$), indicating that encapsulation of fisetin in MPEG−PCL micelles improved fisetin-induced apoptosis of the late stage in CT26 cells.

3.6. Subcutaneous Tumor Model of CT26 Carcinoma.

Figure 7 displayed the data of the subcutaneous CT26 animal model. For the weight of tumors in each group, Figure 7B suggested that fisetin micelles (0.83 ± 0.28 g) were significantly more competent for inhibiting tumor growth than NS (1.80 ± 0.84 g, $P < 0.05$), blank micelles (1.75 ± 0.77 g, $P < 0.05$), and

DOI: 10.1021/am5066893
ACS Appl. Mater. Interfaces 2015, 7, 534−542

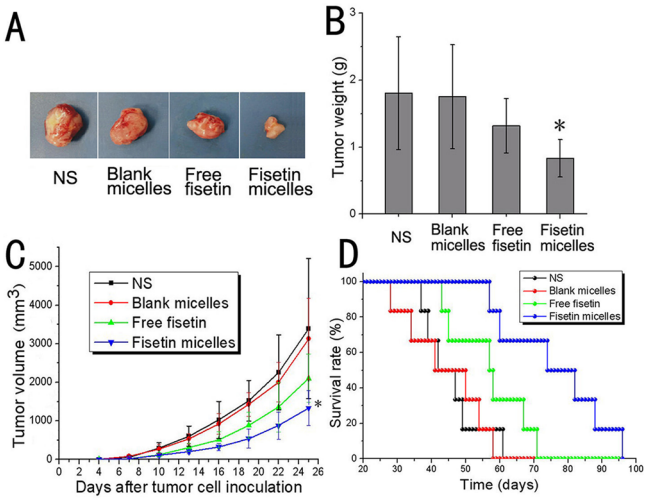

Figure 7. Fisetin micelles inhibited tumor growth in the subcutaneous CT26 model. (A) Representative photographs of subcutaneous tumors in each group. (B) Weight of subcutaneous tumor in each group. (C) Volume of subcutaneous tumors in each group. (D) Survival curves of mice in each group.

free fisetin (1.32 ± 0.41 g, $P < 0.05$) groups. Compared to the NS group, fisetin micelles suppressed the growth of tumors ($P < 0.01$) as Figure 7C showed, while free fisetin did not show significant antitumor activity after day 19 ($P > 0.05$). Tumors in the blank micelles group were not evidently smaller than those in the NS group ($P > 0.05$). Fisetin micelles were more efficient in suppressing growth of tumors than free fisetin ($P < 0.05$). Furthermore, the median survival observation (Figure 7D) indicated that fisetin micelles extended the lifetime of tumor-bearing mice (74 days), compared to NS (42 days, $P < 0.05$), blank micelles (41 days, $P < 0.01$), and free fisetin (57days, $P < 0.05$). In addition, the body weight of mice bearing subcutaneous CT26 carcinoma in each group was measured every 3 days. The body weight of the blank micelles group was not significantly lighter than that of the NS group ($P > 0.05$), suggesting that blank MPEG−PCL micelles would not produce severe systemic toxicity.

3.7. Histological Analysis and Quantitative Assessment of Apoptosis. As for histological analysis (Figure 8), images of H&E stained sections presented that treatment of fisetin could inhibit the malignant proliferation and angiogenesis of tumors. Moreover, fisetin-micelle-treated tissues showed more signs of apoptosis, such as karyopyknosis and apoptotic body.

The apoptosis induction of fisetin micelles on CT26 subcutaneous tumors was investigated by TUNEL immunofluorescent staining assay. We specially chose high-power fields of intact tumor cells to count the TUNEL positive cells (with green fluorescence), so the central necrosis did not interfere with the assessment. Figure 9A to D indicated that much more apoptotic tumor cells existed in tumor tissues treated by fisetin micelles and free fisetin, compared with those in the blank micelles and NS groups. In addition, as shown in Figure 9E, the apoptotic index of the fisetin micelles group (10.08 ± 3.32%) and free fisetin (5.63 ± 1.25%) was significantly higher than that of the NS group (2.50 ± 0.77%, $P < 0.001$), whereas the fisetin micelles group was considered different from that of the free fisetin group ($P < 0.05$). The apoptotic index of the blank

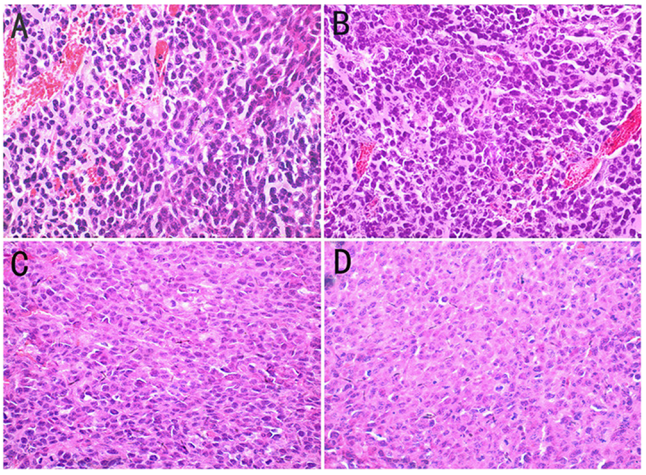

Figure 8. Representative H&E staining images of tumor sections for NS (A), blank micelles (B), free fisetin (C), and the fisetin micelles (D) group.

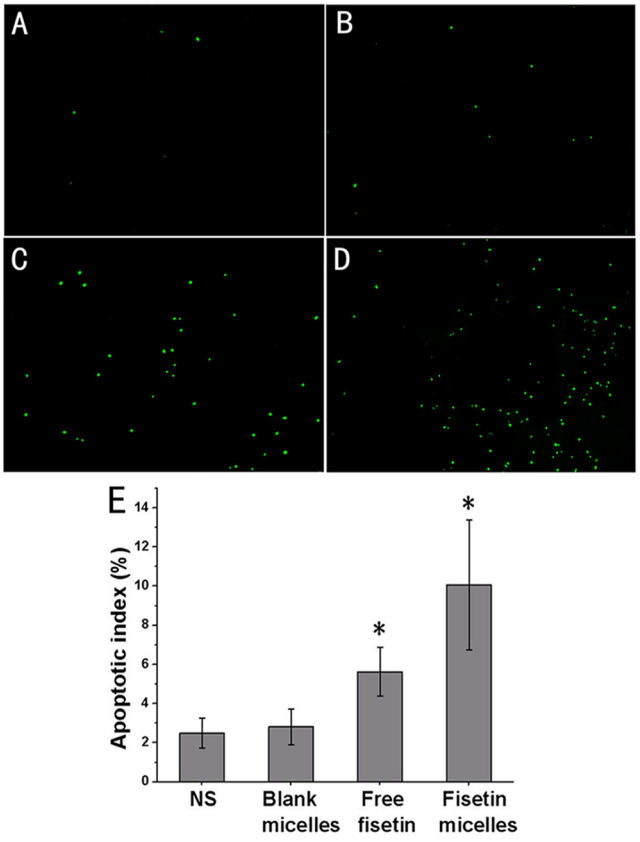

Figure 9. Representative TUNEL immunofluorescent images of tumor sections for NS (A), blank micelles (B), free fisetin (C), and fisetin micelles (D) groups and apoptotic index in each group (E).

micelles group (2.82 ± 0.91%) was not considered different from that of the NS group ($P > 0.05$).

3.8. Immunohistochemical Detection of K_i-67. The proliferation activity of tumor tissues was examined by immunohistochemical detection of K_i-67. Tissues treated by free fisetin (Figure 10C) and fisetin micelles (Figure 10D) contained less K_i-67 positive immunohistochemical staining compared to NS (Figure 10A) and blank micelles (Figure 10B), while fisetin micelles showed an increased efficient antiprolif-

DOI: 10.1021/am5066893
ACS Appl. Mater. Interfaces 2015, 7, 534−542

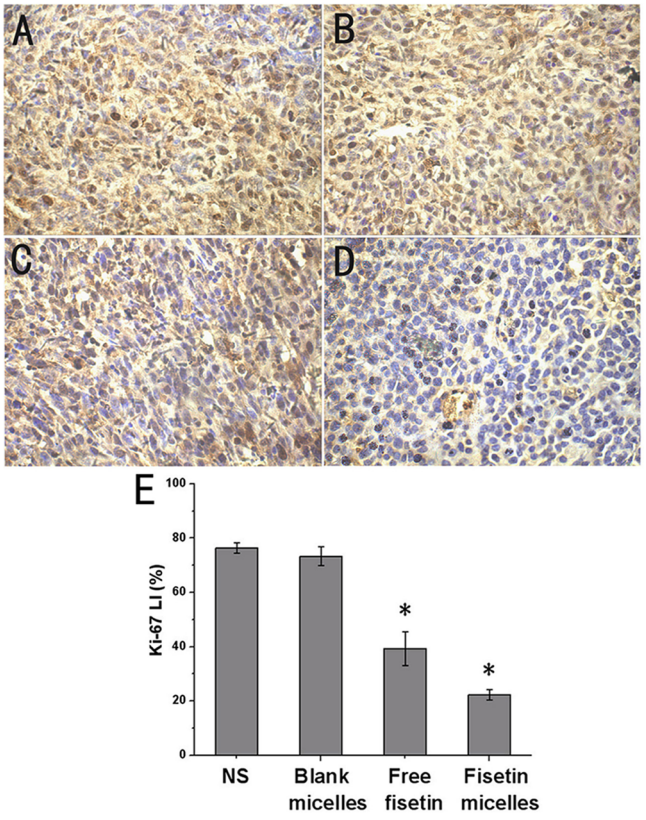

Figure 10. Representative K_i-67 immunohistochemichal images of tumor sections for NS (A), blank micelles (B), free fisetin (C), and fisetin micelles (D) and mean K_i-67 LI in each group (E).

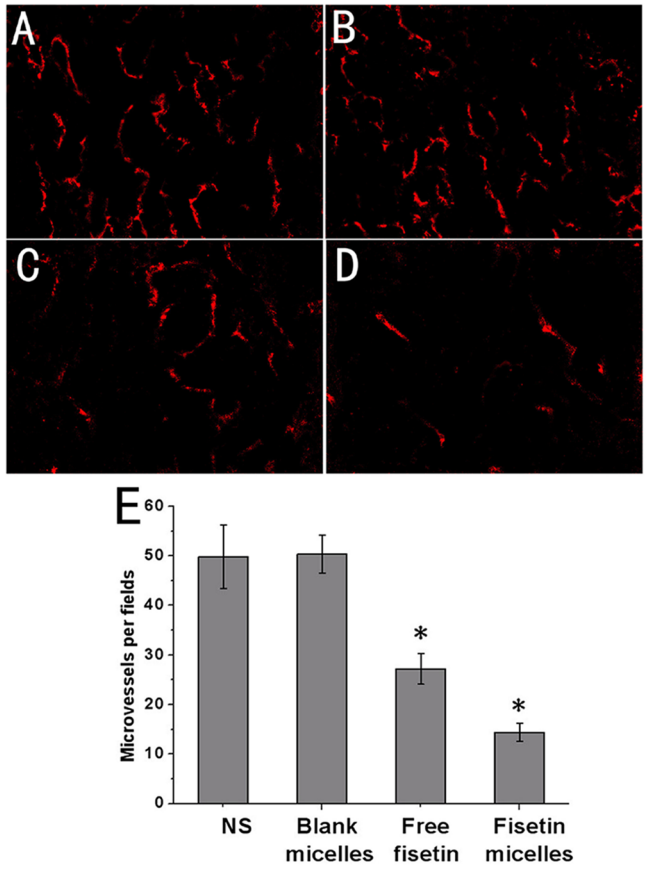

Figure 11. Representative CD31 immunofluorescent images of tumor sections for NS (A), blank micelles (B), free fisetin (C), and fisetin micelles (D) and MVD in each group (E).

eration function compared to free fisetin. According to Figure 10E, K_i-67 LI in the free fisetin group (39.26 ± 6.15%) and fisetin micelles group (22.23 ± 1.96%) was significantly lower than that of the NS group (76.35 ± 1.97%, $P < 0.001$). However, compared to the NS group, the blank micelles group did not show any difference (73.29 ± 3.48%, $P > 0.05$). Moreover, K_i-67 LI in the fisetin micelles group was found to be lower than that in the free fisetin group ($P < 0.001$).

3.9. Immunofluorescence Detection of CD31. As shown in Figure 11A–D, the antiangiogenesis function of fisetin micelles was analyzed by immunofluorescence staining of CD31. Fewer immunoreactive microvessels (red) were observed in tumor tissues treated by free fisetin and fisetin micelles, compared to the NS and blank micelles group. Besides, respectively, in Figure 11E, MVDs in fisetin micelles (14.4 ± 1.8) and the free fisetin group (27.2 ± 3.1) were significantly lower than those in NS (49.8 ± 6.4, $P < 0.001$) and the blank micelles group (50.4 ± 3.8, $P < 0.001$). Moreover, MVD in tissues treated by fisetin micelles was significantly different from tissues treated by free fisetin ($P < 0.001$), indicating that fisetin micelles had enhanced antiangiogenesis activity.

4. DISCUSSION

Nowadays, there are good prospects for natural derived chemotherapeutic agents because those small molecular drugs have more structural diversities, biologically friendly qualities,[29−31] and less limitations due to sourcing problems.[32] The highly anticipated fisetin is recognized as potentially valuable in chemotherapeutic applications. Fortunately, MPEG−PCL micelles are able to solve the problem of fisetin's poor water solubility.

In our previous work, different approaches were made to prepare fisetin micelles, and rotary evaporation with ethanol was finally chosen and employed, with products of excellent properties. The fisetin concentration in aqueous solvent could become much higher. It is considerable to find out that MPEG−PCL encapsulating fisetin showed small particle size (22.4 ± 3.0 nm), good homogeneity (a mean PDI of 0.163 ± 0.032), high EE (98.53 ± 0.02%), and high DL (9.88 ± 0.14%), as well as lasting *in vitro* release behavior. What's more, the surface charge of fisetin micelles was nearly neutral (zeta potential is −3.61 ± 0.24 mV), thus a stereospecific blockade should contribute to the stability of fisetin micelles.

In our study, the superiority of fisetin micelles was confirmed comprehensively and accurately both *in vitro* and *in vivo*. A cytotoxicity study suggested that fisetin micelles had enhanced cytotoxicity compared to free drug (mean IC50 = 7.968 versus 28.513 μg/mL, $P < 0.001$). Apart from that, cells treated by fisetin micelles also exhibited stronger fisetin-induced apoptosis. Both of them might be dependent on the enhanced amount of fisetin taken up by CT26 cells, shown as small dots with green fluorescence (Figure 4A), resulting from the MPEG−PCL package. It was indicated that the uptake mechanisms of fisetin micelles could be connected to some subcellular structures like lysosomes.[33] *In vivo* studies further proved that fisetin micelles possessed a more efficient therapeutic effect (better tumor inhibition and prolonged survivals). Tumor sections were analyzed by H&E staining, TUNEL assay, immunohistochem-

DOI: 10.1021/am5066893
ACS Appl. Mater. Interfaces 2015, 7, 534−542

ical detection of cell proliferation, and immunofluorescence detection of MVD, illustrating that in comparison with free fisetin fisetin micelles had enhanced apoptosis induction, antiproliferation, and angiogenesis effects in the animal model.

Therefore, it is not difficult to recognize that the micelle-based drug carriers for fisetin have brilliant advantages in administration practice. The *in vitro* release study successfully stimulated the procedure that chemotherapeutic agents pass through the blood vessel walls toward tissues.[34] The distinctive different release behaviors of fisetin micelles and free fisetin indicated that drugs encapsulated in micelles could release in circulation at a stable speed. Thus, the drug concentration in plasma could be kept at a relatively stable level to guarantee enough amount of drug would reach the tumor tissues. Besides, the limited release to normal tissues reduced the systemic toxicity of fisetin. In addition, the EPR effect must be referenced. Blood vessels are essential elements of oxygen support and waste transportation in tumor tissues. Different from normal tissues, blood vessels in tumor tissues have a leaky vascular architecture. The gaps between adjacent endothelial cells are large enough (20−2000 nm) for polymer micelles to penetrate. Together with the poor lymphatic drainage of tumors, it is easier for nanoscale particles to extravasate into extravascular spaces and accumulate in tumor tissues.[21] The endothelial cells in normal tissues are connected by tight junctions and less permeable for nanosized particles, which contribute to "passive targeting".[35] Consequently, fisetin micelles can obtain enhanced therapeutic effect and better targeting.

The effectiveness of fisetin micelles has been successfully proved in our study, which makes fisetin micelles a promising source for colon cancer therapy with high antitumor activity and low systemic toxicity. Although there are still needs for further investigations, the excellent properties of fisetin micelles should be taken into consideration for future chemotherapeutic applications.

5. CONCLUSIONS

In this study, biodegradable fisetin micelles have been successfully prepared and applied to the CT26 tumor model *in vitro* and *in vivo*. Compared to free fisetin, fisetin micelles of small particle size and good homogeneity demonstrated lasting *in vitro* release behavior, enhanced cytotoxicity, and cellular uptake, as well as improved apoptosis induction. In the CT26 subcutaneous tumor model, fisetin micelles were more effective in suppressing tumor growth and prolonging survival than free fisetin. Therefore, polymeric micelles encapsulating fisetin with enhanced antitumor activity may become a brilliant aqueous formulation for intravenous application of future colon cancer therapy.

AUTHOR INFORMATION

Corresponding Authors

*Tel.: 86-28-85164063. Fax: 86-28-85164060. E-mail: chygong14@163.com

*E-mail: beggarscn@yahoo.com.cn.

Author Contributions

§These authors contributed equally.

Notes

The authors declare no competing financial interest.

ACKNOWLEDGMENTS

This work was financially supported by Distinguished Young Scholars of Sichuan University (2013SCU04A16), National Natural Science Foundation of China (NSFC81201724), and Specialized Research Fund for the Doctoral Program of Higher Education (20120181120044).

ABBREVIATIONS

MPEG−PCL, monomethyl poly(ethylene glycol)−poly(ε-caprolactone); DDS, drug delivery system; PDI, polydisperse index; DL, drug loading; EE, encapsulation efficiency; TUNEL, terminal deoxynucleotidyl transferase-mediated nick-end labeling; MVD, microvessel density; MTT, thiazoyl blue tetrazolium bromide; PI, propidium iodide; ATCC, American Type Culture Collection; FBS, fetal bovine serum; NS, normal saline; TEM, transmission electron microscope; HPLC, high performance liquid chromatography; FCM, flow cytometry; H&E, hematoxylin and eosin

REFERENCES

(1) Newman, D. J.; Cragg, G. M. Natural Products as Sources of New Drugs over the Last 25 Years. *J. Nat. Prod.* **2007**, *70*, 461−477.

(2) Kimira, M.; Arai, Y.; Shimoi, K.; Watanabe, S. Japanese Intake of Flavonoids and Isoflavonoids from Foods. *J. Epidemiol.* **1998**, *8*, 168−175.

(3) Arai, Y.; Watanabe, S.; Kimira, M.; Shimoi, K.; Mochizuki, R.; Kinae, N. Dietary Intakes of Flavonols, Flavones and Isoflavones by Japanese Women and the Inverse Correlation between Quercetin Intake and Plasma LDL Cholesterol Concentration. *J. Nutr.* **2000**, *130*, 2243−2250.

(4) Ishige, K.; Schubert, D.; Sagara, Y. Flavonoids Protect Neuronal Cells from Oxidative Stress by Three Distinct Mechanisms. *Free Radical Biol. Med.* **2001**, *30*, 433−446.

(5) Park, H.-H.; Lee, S.; Oh, J.-M.; Lee, M.-S.; Yoon, K.-H.; Park, B. H.; Kim, J. W.; Song, H.; Kim, S.-H. Anti-inflammatory Activity of Fisetin in Human Mast Cells (HMC-1). *Pharmacol. Res.* **2007**, *55*, 31−37.

(6) Raygude, K. S.; Kandhare, A. D.; Ghosh, P.; Bodhankar, S. L. Anticonvulsant Effect of Fisetin by Modulation of Endogenous Biomarkers. *Biomed. Prev. Nutr.* **2012**, *2*, 215−222.

(7) Ragelle, H.; Crauste-Manciet, S.; Seguin, J.; Brossard, D.; Scherman, D.; Arnaud, P.; Chabot, G. G. Nanoemulsion Formulation of Fisetin Improves Bioavailability and Antitumour Activity in Mice. *Int. J. Pharm.* **2012**, *427*, 452−459.

(8) Khan, N.; Asim, M.; Afaq, F.; Zaid, M. A.; Mukhtar, H. A Novel Dietary Flavonoid Fisetin Inhibits Androgen Receptor Signaling and Tumor Growth in Athymic Nude Mice. *Cancer Res.* **2008**, *68*, 8555−8563.

(9) Chien, C.-S.; Shen, K.-H.; Huang, J.-S.; Ko, S.-C.; Shih, Y.-W. Antimetastatic Potential of Fisetin Involves Inactivation of the PI3K/Akt and JNK Signaling Pathways with Downregulation of MMP-2/9 Expressions in Prostate Cancer PC-3 cells. *Mol. Cell. Biochem.* **2010**, *333*, 169−180.

(10) Bhat, T. A.; Nambiar, D.; Pal, A.; Agarwal, R.; Singh, R. P. Fisetin Inhibits Various Attributes of Angiogenesis In Vitro and In Vivo Implications for Angioprevention. *Carcinogenesis* **2012**, *33*, 385−393.

(11) Suh, Y.; Afaq, F.; Johnson, J. J.; Mukhtar, H. A Plant Flavonoid Fisetin Induces Apoptosis in Colon Cancer Cells by Inhibition of COX2 and Wnt/EGFR/NF-κB-signaling Pathways. *Carcinogenesis* **2009**, *30*, 300−307.

(12) Chen, W.-S.; Lee, Y.-J.; Yu, Y.-C.; Hsaio, C.-H.; Yen, J.-H.; Yu, S.-H.; Tsai, Y.-J.; Chiu, S.-J. Enhancement of p53-mutant Human Colorectal Cancer Cells Radiosensitivity by Flavonoid Fisetin. *Int. J. Radiat. Oncol.* **2010**, *77*, 1527−1535.

DOI: 10.1021/am5066893
ACS Appl. Mater. Interfaces 2015, 7, 534−542

(13) Lu, X.; Cho, H. J.; Lee, H. S.; Chun, H. S.; Kwon, D. Y.; Park, J. H. Fisetin Inhibits the Activities of Cyclin-dependent Kinases Leading to Cell Cycle Arrest in HT-29 Human Colon Cancer Cells. *J. Nutr.* **2005**, *135*, 2884−2890.
(14) Kedar, U.; Phutane, P.; Shidhaye, S.; Kadam, V. Advances in Polymeric Micelles for Drug Delivery and Tumor Targeting. *Nanomedicine (N. Y., NY, U. S.)* **2010**, *6*, 714−729.
(15) Primeau, A. J.; Rendon, A.; Hedley, D.; Lilge, L.; Tannock, I. F. The Distribution of the Anticancer Drug Doxorubicin in Relation to Blood Vessels in Solid Tumors. *Clin. Cancer Res.* **2005**, *11*, 8782−8788.
(16) de Mendoza, A. E.-H.; Campanero, M. A.; Mollinedo, F.; Blanco-Prieto, M. J. Lipid Nanomedicines for Anticancer Drug Therapy. *J. Biomed. Nanotechnol.* **2009**, *5*, 323−343.
(17) Yallapu, M. M.; Jaggi, M.; Chauhan, S. C. Curcumin Nanoformulations: A Future Nanomedicine for Cancer. *Drug Discovery Today* **2012**, *17*, 71−80.
(18) Oerlemans, C.; Bult, W.; Bos, M.; Storm, G.; Nijsen, J. F. W.; Hennink, W. E. Polymeric Micelles in Anticancer Therapy: Targeting, Imaging and Triggered Release. *Pharm. Res.* **2010**, *27*, 2569−2589.
(19) Singh, M.; Bhatnagar, P.; Srivastava, A. K.; Kumar, P.; Shukla, Y.; Gupta, K. C. Enhancement of Cancer Chemosensitization Potential of Cisplatin by Tea Polyphenols Poly (lactide-co-glycolide) Nanoparticles. *J. Biomed. Nanotechnol.* **2011**, *7*, 202−202.
(20) Saxena, V.; Hussain, M. D. Polymeric Mixed Micelles for Delivery of Curcumin to Multidrug Resistant Ovarian Cancer. *J. Biomed. Nanotechnol.* **2013**, *9*, 1146−1154.
(21) Fang, J.; Nakamura, H.; Maeda, H. The EPR effect: Unique Features of Tumor Blood Vessels for Drug Delivery, Factors Involved, and Limitations and Augmentation of the Effect. *Adv. Drug Delivery Rev.* **2011**, *63*, 136−151.
(22) Gong, C.; Xie, Y.; Wu, Q.; Wang, Y.; Deng, S.; Xiong, D.; Liu, L.; Xiang, M.; Qian, Z.; Wei, Y. Improving Anti-tumor Activity with Polymeric Micelles Entrapping Paclitaxel in Pulmonary Carcinoma. *Nanoscale* **2012**, *4*, 6004−6017.
(23) Fang, F.; Gong, C.; Qian, Z.; Zhang, X.; Gou, M.; You, C.; Zhou, L.; Liu, J.; Zhang, Y.; Guo, G. Honokiol Nanoparticles in Thermosensitive Hydrogel: Therapeutic Effects on Malignant Pleural Effusion. *ACS Nano* **2009**, *3*, 4080−4088.
(24) Gong, C.; Wang, C.; Wang, Y.; Wu, Q.; Zhang, D.; Luo, F.; Qian, Z. Efficient Inhibition of Colorectal Peritoneal Carcinomatosis by Drug Loaded Micelles in Thermosensitive Hydrogel Composites. *Nanoscale* **2012**, *4*, 3095−3104.
(25) Gong, C.; Yang, B.; Qian, Z.; Zhao, X.; Wu, Q.; Qi, X.; Wang, Y.; Guo, G.; Kan, B.; Luo, F. Improving Intraperitoneal Chemotherapeutic Effect and Preventing Postsurgical Adhesions Simultaneously with Biodegradable Micelles. *Nanomedicine (N. Y., NY, U. S.)* **2012**, *8*, 963−973.
(26) Ettenberg, S. A.; Rubinstein, Y. R.; Banerjee, P.; Nau, M. M.; Keane, M. M.; Lipkowitz, S. cbl-b Inhibits EGF-receptor-induced Apoptosis by Enhancing Ubiquitination and Degradation of Activated Receptors. *Mol. Cell Biol. Res. Commun.* **1999**, *2*, 111−118.
(27) Halder, J.; Kamat, A. A.; Landen, C. N.; Han, L. Y.; Lutgendorf, S. K.; Lin, Y. G.; Merritt, W. M.; Jennings, N. B.; Chavez-Reyes, A.; Coleman, R. L. Focal Adhesion Kinase Targeting Using In Vivo Short Interfering RNA Delivery in Neutral Liposomes for Ovarian Carcinoma Therapy. *Clin. Cancer Res.* **2006**, *12*, 4916−4924.
(28) Liu, J.-y.; Wei, Y.-q.; Yang, L.; Zhao, X.; Tian, L.; Hou, J.-m.; Niu, T.; Liu, F.; Jiang, Y.; Hu, B.; et al. Immunotherapy of Tumors with Vaccine Based on Quail Homologous Vascular Endothelial Growth Factor Receptor-2. *Blood* **2003**, *102*, 1815−1823.
(29) Bindseil, K. U.; Jakupovic, J.; Wolf, D.; Lavayre, J.; Leboul, J.; van der Pyl, D. Pure Compound Libraries; A New Perspective for Natural Product bBased Drug Discovery. *Drug Discovery Today* **2001**, *6*, 840−847.
(30) Firn, R. D.; Jones, C. G. Natural Products-A Simple Model to Explain Chemical Diversity. *Nat. Prod. Rep.* **2003**, *20*, 382−391.
(31) Vuorela, P.; Leinonen, M.; Saikku, P.; Tammela, P.; Wennberg, T.; Vuorela, H. Natural Products in the Process of Finding New Drug Candidates. *Curr. Med. Chem.* **2004**, *11*, 1375−1389.
(32) Fischbach, M. A.; Walsh, C. Biochemistry: Directing Biosynthesis. *Science* **2006**, *314*, 603−605.
(33) Tang, N.; Du, G.; Wang, N.; Liu, C.; Hang, H.; Liang, W. Improving Penetration in Tumors with Nanoassemblies of Phospholipids and Doxorubicin. *JNCI, J. Natl. Cancer Inst.* **2007**, *99*, 1004−1015.
(34) Prajakta, D.; Ratnesh, J.; Chandan, K.; Suresh, S.; Grace, S.; Meera, V.; Vandana, P. Curcumin Loaded pH-sensitive Nanoparticles for the Treatment of Colon Cancer. *J. Biomed. Nanotechnol.* **2009**, *5*, 445−455.
(35) Park, J.; Wrzesinski, S. H.; Stern, E.; Look, M.; Criscione, J.; Ragheb, R.; Jay, S. M.; Demento, S. L.; Agawu, A.; Limon, P. L. Combination Delivery of TGF-β Inhibitor and IL-2 by Nanoscale Liposomal Polymeric Gels Enhances Tumour Immunotherapy. *Nat. Mater.* **2012**, *11*, 895−905.

DOI: 10.1021/am5066893
ACS Appl. Mater. Interfaces 2015, 7, 534−542